

SIMULATION AND DESIGN OF AN OMNIDIRECTIONAL CATADIOPTRIC STEREO VISION SYSTEM WITH A HYPERBOLIC DOUBLE LOBE MIRROR FOR ENVIRONMENT MAPPING FROM MOBILE ROBOTS

Giuliano G. de Souza, giuliano_msc@gmail.com

José Maurício S. T. Motta, jmmotta@unb.br

Dept. Mechanical Engineering, Faculty of Technology, University of Brasilia, Brasilia-DF, Brazil, 70910-900

Abstract. *This paper presents an omnidirectional catadioptric vision system with a double lobe hyperbolic mirror that produces images of 360° around the environment. The omnidirectional image capacity results from the use of a convex mirror together with a perspective camera. The double lobe hyperbolic mirror allows the acquisition of a pair of stereo images with a single center of projection, without the need to move the system.*

Mapping an unknown environment using an omnidirectional vision system with a common single lobe mirror is normally carried out during the process of acquisition of pairs of stereo images from a mobile robot moving within the environment to get different images of the same environment points together with measuring the robot displacement. The major limitation of the single lobe mirror system is related to the need to know precisely the robot displacement. Besides, the robot displacement cannot avoid the formation of an area of the environment that is not visible in the direction of the robot motion, making impossible to map dynamic environments.

The proposed system described in this article solves the limitations of the single lobe mirror system described above, since the pair of stereo images is acquired instantaneously without the need to move the vision system, allowing mapping of static and dynamic environments and tracking of objects.

Keywords: *Omnidirectional Vision, Hyperbolic Double Lobed Mirrors, Machine Vision, Robot Vision*

1. INTRODUCTION

A catadioptric omnidirectional vision system produces an image display of a 360°-angle around the environment. This image is the result of the combination of a convex mirror with a camera in such a way that the environment is reflected by the mirror in the direction of the camera's optical axis. An image formed by a catadioptric omnidirectional system usually contains more information from the observed environment than the image generated by a conventional camera. The high density of information in the image and its large field of view makes the system more versatile and has attracted the interest of several researchers (Decca, 2004, Gaspar et al, 2001), since the use of only a single camera carried by a mobile robot turns the mapping of a large area of the environment around the robot a feasible task.

Mapping an unknown environment by using a catadioptric omnidirectional vision system with a single lobe mirror can be accomplished from a pair of stereo images acquired during the robot navigation (Bunschoten, 2003). The major limitation of using this type of stereo catadioptric omnidirectional vision system (needs the acquisition of two images at two different positions) is related to the need of a precise robot motion to acquire the pair of stereo images. Besides, the robot motion may move the camera to a place from where it is impossible to the camera to acquire the second image of the same environment region. Other limitations are impossibility of mapping dynamic environments, since there is loss of information during the simultaneous motion of the object and the vision system.

To reduce the limitations of a stereo catadioptric omnidirectional vision system described above a hybrid system may be used (Adorno et al, 2001) by joining both catadioptric omnidirectional and conventional vision systems to generate two different images. Other options are the use of two catadioptric omnidirectional systems (Koyasu et al, 2002) or the use of a catadioptric omnidirectional system with a double-lobe mirror, which is presented in this article as a more compact and economical alternative when compared with the hybrid and double system solutions.

This article proposes an alternative for stereo catadioptric omnidirectional vision systems by adopting a hyperbolic double-lobe mirror to obtain stereo information by acquiring only one image at a location instead of two images from two different places. Furthermore, it is discussed a computer algorithm built specially to process the omnidirectional images to generate 2D maps for robot navigation.

The hyperbolic mirror profile provides a single center of projection, thus eliminating the distortions caused by overlapping images. The use of a double-lobe mirror profile makes possible the acquisition of a pair of stereoscopic images at the same time, allowing the construction of maps from static and dynamic environments without the need to move the vision system.

The algorithm basically extracts image features, such as edge points of objects, and calculates the correlation between equivalent features and triangulates the corresponding features. The algorithm developed proposes a method for matching equivalent features in this task. The method proposed reduces the computational cost and the matching errors.

2 CATADIOPTRIC OMNIDIRECTIONAL VISION SYSTEMS

A catadioptric omnidirectional vision system is composed by a convex mirror in front of a camera in such a way that the mirror in the camera field of view can reflect the surrounded environment. Catadioptric omnidirectional vision systems can be found in a wide range of types, varying from mirror profiles, camera models to lens used.

A mirror profile can vary depending on the application and the technology available to manufacture it. Among several mirrors that can be possibly used, it can be cited the spherical mirror (Vassallo, 2004, Grassi-Jr, 2001), the conical mirror (Yagi, 1999), the parabolic mirror (Nayar, 1997), a mirror designed by Hicks and Bajesy (1999) with a profile with properties that preserve in the image the geometry of a plane perpendicular to mirror symmetry axis, a mirror designed by Gächter et al (2001), with a profile that preserves the dimensions of an object in the image when it moves in a vertical plane, and the hyperbolic mirror (Bunschoten, 2003, Correa, 2004).

A catadioptric omnidirectional vision system has as its main advantage the ability of reflecting 360° of the surrounded environment using a single camera. This broad vision enables its application in several areas, such as navigation, visual servo control, teleoperation and environment monitoring. The navigation of mobile robots with the use of such a system allows a high degree of autonomy and has been the focus of various research works (Nayar, 1997, Winters, 2001, Decca, 2004, Svoboda et al., 1997). The limitations of the system are related to the definition of the image obtained, which depends on the profile and surface quality (Souza and Motta, 2007).

3 DESIGN OF THE HYPERBOLIC DOUBLE LOBE MIRROR PROFILE

Hyperbolic mirror profiles have been used by various authors (Decca, 2004, Winters, 2001, Grassi-Jr, 2001) to construct catadioptric omnidirectional vision systems. The main advantage of this profile is that there is only one projection center of the image. When an omnidirectional vision system has a single center of projection, it is assured that the object projections will not produce overlaid images, thus avoiding additional image distortions and blurring.

The 3D reconstruction of the environment from a pair of stereo omnidirectional images by using a single lobe mirror is limited by the potential existence of invisible areas that should be framed by the camera simultaneously in the direction of motion (Correa, 2004) and by the impossibility of mapping dynamic environments.

An omnidirectional vision system with a single lobe mirror needs to be moved to acquire the second image of the stereo pair, which requires that the environment is static such that the objects are imaged in the same location as in the first image. This limitation restricts the use of the system in dynamic environments.

All these drawbacks can be bypassed by using a double-lobe hyperbolic mirror that instantaneously generates a pair of stereo omnidirectional images without the need of sensor measuring of the robot displacements, allowing the calculation of the object position and avoiding the loss of information. The hyperbolic curve is defined by Eq. (1).

$$\frac{(y-k)^2}{a^2} - \frac{(x-j)^2}{b^2} = 1 \tag{1}$$

such that (j, k) is the hyperbole center and the lengths a and b are the hyperbole semi-axes. If the center of the hyperbole coincides with the origin, i.e., j = 0 and k = 0, the hyperbole equation is simplified as Eq. (2).

$$\frac{y^2}{a^2} - \frac{x^2}{b^2} = 1 \tag{2}$$

If the origin of the Cartesian coordinate system is transferred from the point (j, k), to the focus F₂ and the camera focal point coincides with the focus F₂, Fig. (1) shows the association of a hyperbolic mirror with a camera of perspective projection, where the origin coincides with the camera focus point.

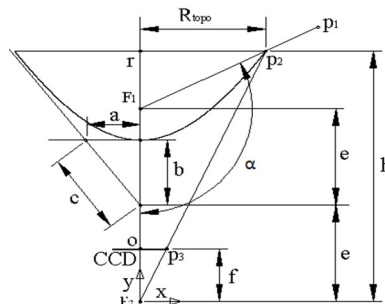


Figure 1. Hyperbolic mirror associated with a perspective projection camera.

In Fig. (1), f is the camera focal length, h is the distance between the edge of the mirror and the camera focus point, R_{top} is the x coordinate of the mirror and α is the maximum angle of view of the system, which is the largest incidence angle of light rays that is reflected on the CCD camera. These parameters are related by the equations that define the hyperbole, Eq (3) and Eq (4), and by the trigonometric relations of the rectangle triangle F_1P_2r , (Eq. (5)).

$$e = \sqrt{a^2 + b^2} \tag{3}$$

$$y = \sqrt{a^2 \cdot \left(1 + \frac{x^2}{b^2}\right)} + e \tag{4}$$

$$\alpha = \frac{\pi}{2} + atan\left(\frac{h-2e}{R_{top}}\right) \tag{5}$$

For the omnidirectional vision system to use the full capacity of the CCD camera and to have a suitable size, one has to find empirically a good relationship between the parameters h and R_{top} , Eq. (6), defined by the relationship between the similar triangles F_2P_2r and F_2P_3O Fig. (1).

$$h = \frac{f \cdot R_{topo}}{T_{pixel} \cdot R_{pixel}} \tag{6}$$

In Eq.(6), R_{pixel} is the largest radius of the circle that can be inscribed in the CCD camera (in pixels), Fig. (2), and T_{pixel} is the size of each pixel of the CCD camera (in millimeters).

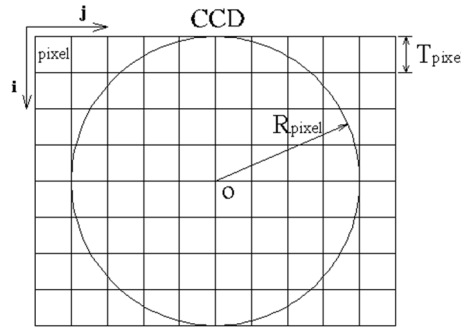


Figure 2. CCD camera.

To calculate the points that define the hyperbolic mirror profile, Eq. (4) is used. This equation is dependent on the lengths a and b , which are related by the eccentricity c of hyperbole Eq. (7).

$$c = \frac{a}{b} \tag{7}$$

Replacing the coordinates (R_{top}, h) of point P_2 of the hyperbole, Fig. (1), and using Eq. (3) in the equation that defines the hyperbolic curve (Eq. (4)) and working mathematically with this equation Eq. (9) and Eq. (10) it is possible to calculate a quadratic equation for the parameter b .

$$h = \sqrt{a^2 \left(1 + \frac{R_{top}^2}{b^2}\right)} + \sqrt{a^2 + b^2} \tag{8}$$

$$h = \frac{a}{b} \sqrt{b^2 + R_{top}^2} + b \sqrt{\frac{a^2}{b^2} + 1} \tag{9}$$

$$\left(\frac{a}{b} \sqrt{b^2 + R_{top}^2}\right)^2 = \left(h - b \sqrt{\frac{a^2}{b^2} + 1}\right)^2 \tag{10}$$

$$b^2 - b \left(2h \sqrt{\frac{a^2}{b^2} + 1} \right) + \left(-\frac{a^2}{b^2} R_{top}^2 + h^2 \right) = 0 \quad (11)$$

The solution of Eq. (11) yields Eq. (12), which expresses the length b as a function of the ratio a/b.

$$b = h \sqrt{\frac{a^2}{b^2} + 1} - \frac{a}{b} \sqrt{h^2 + R_{top}^2} \quad (12)$$

Replacing Eq. (7) in Eq. (12), the equation that expresses the parameter b as a function of eccentricity c is:

$$b = h \sqrt{c^2 + 1} - c \sqrt{h^2 + R_{top}^2} \quad (13)$$

Parameter c has influence on the hyperbolic curve profile and therefore in the field of view of the system. The lower mirror (Mir₁), Fig. (3), with focus F_{1,1} has the region A as its field of view and the upper mirror (Mir₂) with focus F_{1,2} has region B as its field of view. For the determination of c of each mirror, various values for c₁ and c₂ were tested and the optimal result obtained was the one with the larger intersection region, AB, in the field of view, optimizing the use of the camera CCD area. Another factor that influences the choices of parameters c₁ and c₂ is the distance between the focal points F_{1,1} and F_{1,2}, since the larger is the distance between them smaller is the sensitivity to errors during the image processing. However, if the distance is too large the system is enlarged and may be unable to be embedded onto a mobile robot. The optimal values obtained were c₁ = 1.5 and c₂ = 0.9 for the bottom mirror (Mir₁) and top mirror (Mir₂).

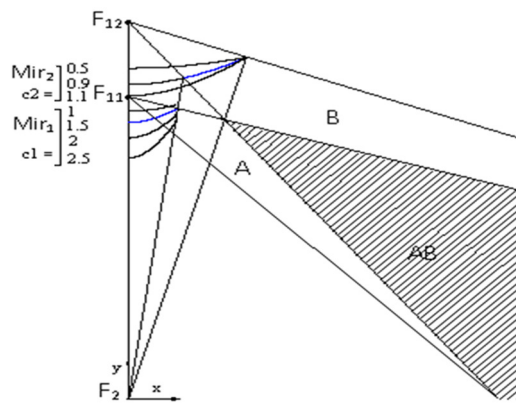


Figure 3. Variations in the mirror profiles.

To calculate the points that define each profile a computer program in C language was developed based on the equations already shown. The program calculates the points and represents them in Cartesian coordinates. In theory, the more points are available and more they approach the ideal profile, the better is the quality of the mirror surface. In practice, the number of points will be limited by the accuracy and the storage capacity of the control system of the machine tool used to manufacture the mirror.

The equations used in the computer program routines are Eq. (3) - (7) and Eq. (13), forming an underdetermined system with 6 equations and 10 unknowns. Some of these unknowns were set up as constant parameters to enlarge the used area of the camera CCD and the environment area framed by the camera optics (Fig. (4)), where Mir₁ is the lower lobe surface and reflects the image region A, Mir₂ is the upper lobe surface and reflects the image region B. The intersection of these two regions forms the region AB, which is reflected by the two lobes of the mirror, forming the pair of stereo images. The regions that are not part of the intersection will be discarded during the image processing. As an example, one can choose the values R_{top1} = 25 mm, R_{top2} = 60 mm, f = 16 mm and T_{pixel} = 0.009 mm. The CCD camera is a square of 1008 x 1008 pixels, making R_{pixel2} = 504. R_{pixel1} was calculated from

$$R_{pixel1} = \frac{R_{pixel2} - \frac{R_{pixel2} \cdot Sf}{2}}{T_{pixel}} \quad (14)$$

Equation (14) is formulated to optimize the use of the CCD camera, where the SH is the shadow caused by the reflection of the camera and can be defined as SH = 1mm, for this case.

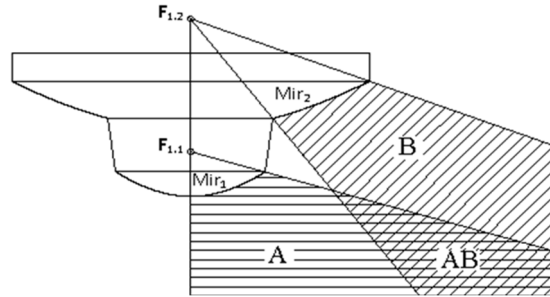


Figure 4. Projected profile of the double lobe mirror.

Setting up the above parameters and running the computer routine developed, the other parameters needed for the mirror design were calculated and are shown in Table (1).

Table 1. Parameters of the proposed vision system.

CONSTANT INPUT PARAMETERS				CALCULATED PARAMETERS					
Mir	R_{top} (mm)	T_{pixel} (mm)	R_{pixel} (pixel)	c	h (mm)	$2e$ (mm)	a (mm)	b (mm)	α
1	25	0,009	307	1,5	184,97	187,07	77,83	51,88	86°
2	60	0,009	504	0,9	211,64	233,42	78,08	86,75	70°

Using the parameters calculated above in Eq (4), two equations are generated, Eq. (15) and Eq (16), defining the hyperbolic profiles 1 and 2, respectively:

$$y_1 = \sqrt{77,825^2 \cdot \left(1 + \frac{x_1^2}{51,883^2} \right)} + 93,534 \quad (15)$$

$$y_2 = \sqrt{78,075^2 \cdot \left(1 + \frac{x_2^2}{86,750^2} \right)} + 116,71 \quad (16)$$

Using Eqs. (15) and (16) and increasing x_1 and x_2 by 0.005 mm, 5,000 points were calculated for the profile 1 and 6,600 points for the profile 2, as shown in Fig. (5, b). For a better view of the mirror a 3D model was built using the AutoCAD™ software Fig. (5, a), whose parameters are shown in Table (1).

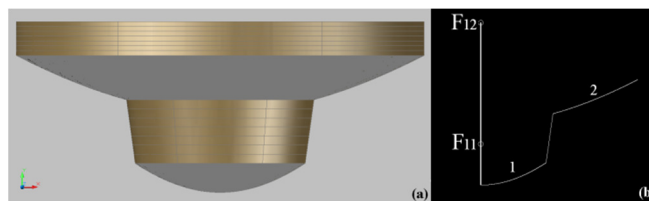


Figure 5. Double lobe hyperbolic mirror: (a) revolution of the mirror profile; (b) mirror profile.

4 SIMULATION OF THE IMAGE ACQUISITION PROCESS

The construction of an omnidirectional vision system with a hyperbolic mirror is complex and requires high precision mirror modeling and manufacturing. A wrong choice of the parameters that define the mirror profile may produce images including unnecessary environment regions, as a result of unpredicted field of views. As the proposed mirror has two lobes, this problem is more severe because the area of interest must be reflected by two mirror profiles

which form a pair of concentric and radial stereo images, in such a way that the images shall not have overlapping areas on the camera CDD.

The main purpose of the simulation of the image acquisition process is to test the mirror profile eventually designed. Concerning the reliability of this technique, the simulation is performed in a virtual environment with known dimensions. The computer routine developed was compiled with the aid of POV-Ray, which is free computer software that allows the creation of realistic 3D images with high dimensional precision.

The virtual camera conceived to generate the 3D images is to keep the same parameters used to design the mirror profile, i.e. a camera with perspective projection and focus length $f = 16\text{mm}$ and rectangular CCD of 1008×1008 pixels.

The illumination was adjusted such that the environment receives uniform light incidence. Then four light sources were established to be placed in each corner of the board at a height of 3m from the ground.

The environment to be simulated consists in an area of 800×800 mm containing a black and white squared grid of 50×50 mm, created with the software routines to define plans and textures. In Fig. (6) it is shown the result of the generated image of the environment reflected in the mirror.

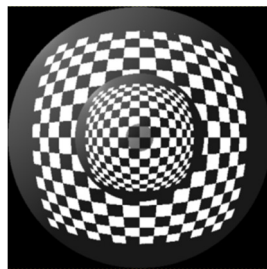


Figure 6. Omnidirectional Image re-scaled to 1008×1008 pixels.

5 SIMULATION OF THE ENVIRONMENT MAP

For a mobile robot to navigate around an unknown environment certain features must be extracted by the sensor system for it to be able to precisely locate objects within that environment. One way to do that in a particular region is to make use of a map, which should assign some level of uncertainty to sizes and locations of potential obstacles. In this section, a method to simulate this mapping process by using a catadioptric omnidirectional stereo image system is discussed. This method is based on common procedures used in stereoscopic vision, such as the selection of the type of feature that should be observed in the environment image, the location of the pairs of correspondent features and the construction of the map by using triangulation between these features.

Initially, the system performs the extraction of features from the image, which in this case are the contours of objects within an environment region. Edge detection is normally a low-level operation to extract features by using gradient-based algorithms to detect changes in brightness in the image. To generate an image with sharp edges, Fig. (7), a Prewitt operator was used, since it is an efficient and simple filter, reducing processing time in dynamic environments. Subsequently the image is submitted to a binarization process to reduce false contours.

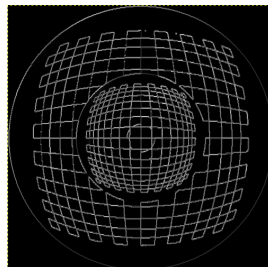


Figure 7. Processed Image.

One of the important steps of stereoscopic image processing is the correspondence searching of pairs of features, i.e. to identify the point C_1 when C_2 is known, Fig. (8). An important characteristic of the double lobe hyperbolic mirror system is that the corresponding point C_1 always belongs to a radial line that links the point O with point C_2 . This makes the identification easier since the search by the corresponding point is limited to straight line OC_2 .

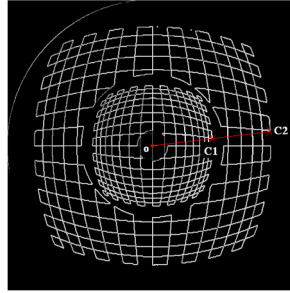


Figure 8. Correspondent Points.

The identification of corresponding pair of points makes use of a cost function which calculates the sum of the square differences (SSD) between two search windows M1 and M2 Fig. (9), in which the centers of the windows are the points to be compared, c_1 and c_2 , and the other elements of the matrices are neighborhoods of the points.

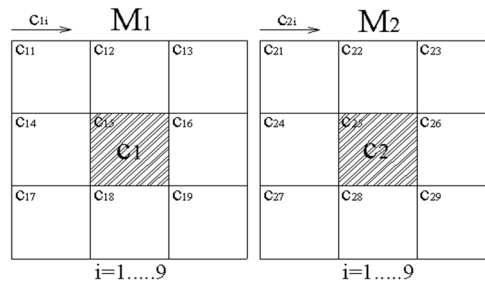


Figure 9. Sum of the square differences windows

Firstly, a point of interest c_2 is established and so the window size, i . Subsequently, a candidate correspondent point c_1 is selected during the search process and the SSD is calculated by Eq. (17). This operation is performed for all likely correspondent points, and the smallest value is taken as the corresponding point. This method can generate errors, which are enlarged as much as there is homogeneity in the gray intensity levels of the image pixels, since the more homogenous is the image, higher is the probability of existing points with similar SSD values. To reduce this problem one can choose a mask with larger size or with specific formats.

$$SSD = \sum_{i=1}^n (c_{1i} - c_{2i})^2 \tag{17}$$

In the system developed, the image generated by the mirror 1 is smaller than that generated by the mirror 2, which means that the same object has different image scales for each mirror, turning the square shaped window ineffective to identify the correspondent point. In this article, it is proposed a method that uses a circular window, Fig. (10), where each neighbor pixel is at an angle θ relative to the previous one. As smaller is θ (fixed parameter), the larger is the number of neighbor points and better is the outcome, therefore increasing the processing time. In this work, $\theta = 0,1$ radians, chosen as an interval within an angle range of 2π , which produces a window with 60 cells ($n = 60$).

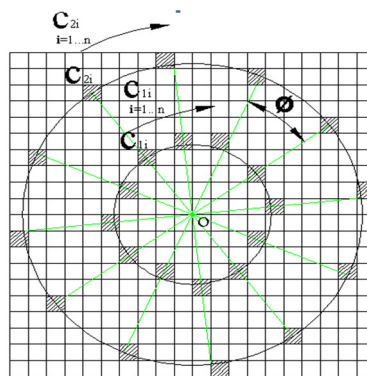


Figure 10. Radial model of the sum of the square difference windows.

To implement the system, a routine in C language was developed and to test this program a simulation was carried out to identify the pairs of equivalent points. In the simulation, the binary image generated in the previous section was used. The image was divided into two areas (Fig. 11a), i. e. the first, I_1 , bounded by circles of rays R_1 and R_2 and the second, I_2 , bounded by circles R_3 and R_4 . Initially, the pixels with values equal to 255 (white) were identified in the area I_2 and for each identified pixel a corresponding pixel belonging to the area I_1 was found. Next to identification of correspondent points, an image was created with the calculated coordinates (Fig. 11b).

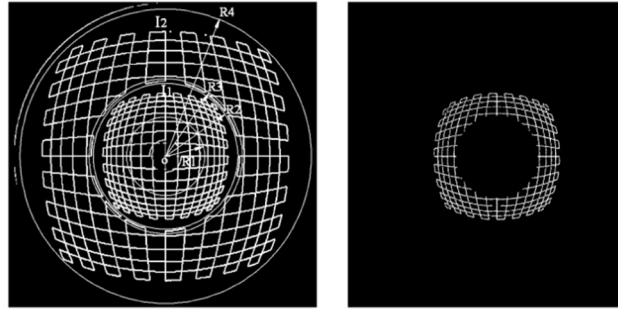


Figure 11. Determination of the equivalent points: (a) scanning areas; (b) equivalent points.

For each supposed correspondent pair of points C_1 and C_2 found, the coordinates (X, Y) of point P (Fig. 12a) at the environment are calculated. The coordinates of point P will be calculated from the trigonometric equations formulated from the similar triangles in figure (12a), to be detailed further in the text.

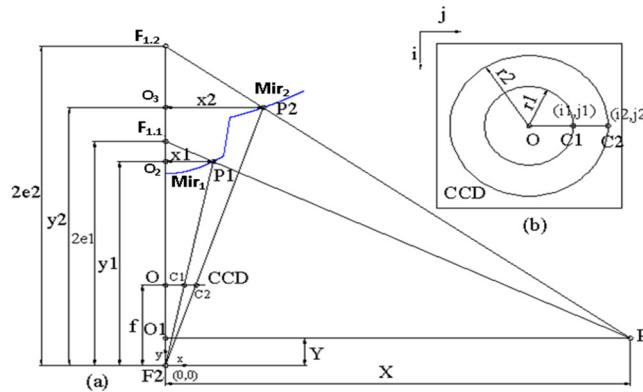


Figure 12. Environment coordinate point: (a) triangulation; camera CCD.

Initially, the radius of the circles, r_1 and r_2 , were calculated, whose points C_1 and C_2 belong to Fig (12b), that means, the segments OC_1 and OC_2 respectively. Thus, triangle relationships were used as in Eq. (18) and Eq (19).

$$r_1 = OC_1 = \sqrt{\left(\frac{height}{2} - i_1\right)^2 + \left(j_1 - \frac{width}{2}\right)^2} \quad (18)$$

$$r_2 = OC_2 = \sqrt{\left(\frac{height}{2} - i_2\right)^2 + \left(j_2 - \frac{width}{2}\right)^2} \quad (19)$$

As triangle F_2OC_1 is similar to the triangle $F_2O_2P_1$ and triangle F_2OC_2 is similar to the triangle $F_2O_3P_2$, it is possible to relate the x_1 with y_1 and x_2 with y_2 , as in Eq. (20) and Eq. (21) respectively.

$$\frac{y_1}{f} = \frac{x_1}{r_1} \quad (20)$$

$$\frac{y_2}{f} = \frac{x_2}{r_2} \quad (21)$$

The equations (22) and (23) below are obtained merging Eq. (20) with Eq. (4), producing the mirror 1 profile. Equations (24) and (25) are obtained merging Eq. (21) with Eq. (4), producing the mirror 2 profile. With these equations it is possible to calculate the coordinates of the points P1 (x_1, y_1) and P2 (x_2, y_2).

$$x_1 = \frac{\left(f e_1 b_1 + a_1 \sqrt{f^2 b_1^2 + r_1^2 e_1^2 - a_1^2 r_1^2} \right) b_1 r_1}{f^2 b_1^2 - a_1^2 r_1^2} \quad (22)$$

$$y_1 = \frac{x_1 f}{r_1} \quad (23)$$

$$x_2 = \frac{\left(f e_2 b_2 + a_2 \sqrt{f^2 b_2^2 + r_2^2 e_2^2 - a_2^2 r_2^2} \right) b_2 r_2}{f^2 b_2^2 - a_2^2 r_2^2} \quad (24)$$

$$y_2 = \frac{x_2 f}{r_2} \quad (25)$$

Triangle $F_{11}PO_1$ is similar to the triangle $F_{11}P_1O_2$ and triangle $F_{12}PO_1$ is similar to the triangle $F_{12}P_2O_3$. Using similar triangles relationships the equations that relate the coordinates of the point P (X, Y) with the coordinates of the point P1 (x_1, y_1) and P2 (x_2, y_2) are derived as Eq. (26) and Eq. (27) respectively.

$$\frac{X}{x_1} = \frac{2 e_1 - Y}{2 e_1 - y_1} \quad (26)$$

$$\frac{X}{x_2} = \frac{2 e_2 - Y}{2 e_2 - y_2} \quad (27)$$

The combination of Eq. (26) with Eq. (27) yields Eq. (28) and Eq. (29), producing the coordinates of point P.

$$X = \frac{2 x_1 x_2 (e_2 - e_1)}{x_1 (2 e_2 - y_2) - x_2 (2 e_1 - y_1)} \quad (28)$$

$$Y = \frac{2 e_2 - X (2 e_2 - y_2)}{x_2} \quad (29)$$

For each pair of correspondent points the computer program developed calculates the coordinates (X,Y) of the corner points of an object within the environment, making possible the creation of an environment map.

The X coordinate of point P (X, Y) is transformed into vector r_2 with origin at the center of the map and same angle of inclination with respect to the abscissas' axis. The map consists of a square matrix with 1008 x 1008 cells, in which each cell corresponds to an area of 1 mm² of the viewed environment. With all the coordinate points calculated a map can be constructed as in Fig. (14a). By overlaying the map calculated on the ideal map, as shown in Fig. (14b), it is possible to identify the dispersion of the points that should compose the lines of the calculated map.

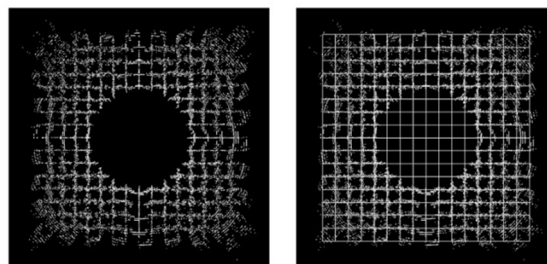


Figure 14. Mapping: (a) calculated map; (b) superposition of the ideal and calculated maps.

6 Conclusions

In this work, a simulation was carried out aiming at mapping an environment with the use of a catadioptric omnidirectional vision system with a double lobe hyperbolic mirror. The use of this special type of mirror makes possible the creation of two instant images of the environment as viewed from different camera positions due to the two mirror profiles, forming a pair of stereo images without the need to move the system. The simulation of the mapping process was performed with a high geometric precision and with a series of programs specially developed in C language. The parameters used to develop the model were chosen to allow the construction of small-sized equipment that can be used for mobile robot navigation.

The image processing routines were conceived to use the object contours within the environment as image features to be identified and located. Since the identification of the features was performed point by point, it could be expected that the map generated was to be composed by a set of scattered points. This dispersion depends on the errors generated during the image processing.

The map generated from the pair of stereo images is formed by a cloud of scattered points. The dispersion of points is dependent on the system accuracy in such a way that the less dispersed are the map points the better can be the results. With the aid of appropriate software it is possible to quantify the dispersion of the map points and replace the cloud of points with a curve that approaches the ideal. This can be checked with the map overlay on the ideal map.

Finally, the developed system used a pair of stereo images obtained instantaneously without the need to move the system, which allows the mapping of static and dynamic environments and the tracking of moving objects. The map generated allows the navigation of mobile robots within the environment in speeds directly related to the speed of acquisition and image processing, which suggests an optimization scheme towards reducing the maximum time for generating the map.

References

- Bunschoten, R., 2003, "Mapping and Localization from a Panoramic Vision Sensor". Doctorate Thesis, Universiteit van Amsterdam.
- Corrêa, F. R., 2004, "Grades De Evidência Com Visão Estéreo Omnidirecional Para Navegação De Robôs Móveis", Master Dissertation, Universidade de São Paulo, 2004.
- Deccó, C. C. G., 2004, "Construção de Mapas de Ambiente para Navegação de Robôs Móveis com Visão Omnidirecional Estéreo". Doctorate Thesis, Escola Politécnica da Universidade de São Paulo.
- Gaspar, J., Deccó, C., Okamoto-Jr., J., Santos-Victor, J., 2002, "Constant Resolution Omnidirecional Cameras", OMNIVIS'02 - Workshop on Omnidirectional Vision, held with ECCV, Copenhagen, Denmark, June 2002.
- Gächter, S.; Pajdla, T.; Micusík, B. M., 2001, "Mirror Desing for an Omnidirectional Camera with a Space Variant Imager". In: Workshop on Omnidirectional Vision Applied to Robotic Orientation and Nondestructive Testing, Budapest, Hungary.
- Grassi-Jr., V., 2002, "Sistema de Visão Omnidirecional Aplicado no Controle de Robôs Móveis", Master Dissertation, Universidade de São Paulo, 2002.
- Grassi-Jr., V., Deccó, C. C. G., Okamoto-Jr., J., Porto, A. J. V., 2001, "Desenvolvimento de Um Sistema de Visão Omnidirecional", 16º Congresso Brasileiro de Engenharia Mecânica, Uberlândia.
- Hicks, A.; Bajcsy, R., 1999, "Reflective Surfaces as Computational Sensors", In: Workshop on Perception for Mobile Agents at CVPR'99, Colorado, USA. Proceeding of CVPR99. Piscataway, Nj: IEEE Computer Press.
- Nayar, S. K., 1997, "Catadioptric Omnidirectional Camera", Proceeding of the IEEE International Conference on Computer Vision and Pattern Recognition, San Juan, Puerto Rico, pp. 482 – 488.
- Winters, N., 2001, "A Holistic Approach to Mobile Robot Navigation Using Omnidirectional Vision". Thesis, Department of Computer Science, University of Dublin, Ireland.
- Svoboda, T. Pajdla, T. Hlavác, V., 1997, "Central Panoramic Câmeras: Geometry and Desing", Tech. Report K335/97/147, Czech Technical University, Faculty Of Electrical Engineering, Department Of Control Engineering, Center For Machine Perception.
- Vassallo, R. F., 2004, "Uso de Mapeamentos Visuo-Motores com Linguagem Omnidirecional para Aprendizagem por Imitação em Robótica", Doctorate Thesis, Universidade Federal do Espírito Santo.
- Souza, G. G.; Motta, J. M., 2007, "Simulation of an Omnidirectional Catadioptric Vision System with Hyperbolic Double Lobed Mirror for Robot Navigation". 19th International Congress of Mechanical Engineering November 5-9, 2007, Brasília, DF.
- Yagi, Y., 1999, "Omnidirectional Sensing and Its Applications". IEICE Transactions on Information and Systems, V.E82-D, N.3, P.568-579.

5. RESPONSIBILITY NOTICE

The authors are the only responsible for the printed material included in this paper.